Structural characteristics of AlN films deposited by pulsed laser deposition and reactive magnetron sputtering: A comparative study

K. Jagannadham, A. K. Sharma, Q. Wei, R. Kalyanraman, and J. Narayan
Department of Materials Science and Engineering, NSF Center for Advanced Materials Processing and Smart Structures, North Carolina State University, Raleigh, North Carolina 27695

(Received 2 February 1998; accepted 26 June 1998)

Aluminum nitride films have been deposited on Si(111) substrates at different substrate temperatures using two techniques; pulsed laser deposition or reactive magnetron sputtering. The films deposited by either of the techniques have been characterized by x-ray diffraction and transmission electron microscopy to determine the crystalline quality, grain size, and epitaxial growth relation with respect to the substrate. The bonding characteristics and the residual stresses present in the films have been evaluated using Raman and Fourier transform infrared spectroscopy. Secondary ion mass spectrometry has been performed to determine the nitrogen stoichiometry and the presence of impurities such as oxygen and silicon. The adhesion strength of the AlN films to the silicon substrate and the wear resistance have been determined by scratch test and a specially designed microscopic wear test. A comparison of the different characteristic features associated with the AlN films deposited by pulsed laser deposition or magnetron sputtering is presented with particular emphasis to electronic and tribological applications. © *1998 American Vacuum Society.* [S0734-2101(98)06305-2]

I. INTRODUCTION

III–V nitrides are potential candidates for optoelectronic applications because of their direct and wide band gaps. Among them, aluminum nitride (AlN) is the most interesting compound[1] with a wide band gap, high values of surface acoustic velocity, thermal conductivity, dielectric constant, and high temperature stability and hardness. AlN is a potential candidate for use in the fabrication of blue light emitting diodes (LED), short wavelength lasers and ultraviolet (UV) light detectors. High quality epitaxial AlN films on suitable substrates are essential for all these applications. AlN has been deposited by several techniques such as metalorganic chemical vapor deposition (MOCVD),[2] plasma-assisted molecular beam epitaxy (MBE),[3] pulsed laser deposition (PLD),[4–8] and reactive magnetron sputtering (RMS).[9–12] Among these techniques, PLD is cited in the literature[13] to have an advantage over others owing to stoichiometric reproduction of the target composition in the films, higher energy (5–10 eV) of the ablated species and higher partial pressures of reactive gases (>10 mTorr) that can be maintained to attain the desired composition. However, presence of particulates of the target material in the laser generated plume and limited size of the substrate for uniform deposition are challenges to be met. An equally promising technique for thin film deposition of insulating nitrides, oxides and carbides is the reactive magnetron sputtering using pulsed dc power. In addition to higher energy of the species (5–10 eV) in the plasma, larger area (8 inch diameter wafer) deposition of the uniform films is carried out using RMS.

Suitable choice of substrates to deposit epitaxial films of AlN are α-Al_2O_3 (0001) and Si(111) favorable for domain matching and ZnO(0002) and SiC(0001) with lattice matching. SiC(0001) is the best lattice matched (3%) substrate for epitaxial growth of AlN(0001). However, we have chosen the Si(111) substrate for deposition of AlN for two reasons: first, the thermal expansion coefficient of AlN matches well with that of silicon and second, silicon is a widely used substrate for electronic applications compared to SiC or α-Al_2O_3.

In this comparative study, we have employed two different techniques of synthesis: PLD and RMS for deposition of AlN films on Si(111) substrates. An important difference between the two methods is that an AlN target is used in the PLD, whereas an aluminum target is utilized in the RMS for reasons mentioned below. The objective of the present investigation is to determine the differences in crystalline quality, relative impurity levels, and tribological properties such as wear and adhesion of the films deposited by PLD and RMS.

II. EXPERIMENTAL PROCEDURE

A. Reactive magnetron sputtering

Aluminum nitride films can be deposited by magnetron sputtering using either an aluminum nitride target or an aluminum target. Because of the dielectric behavior of AlN (resistivity of $10^{13}\ \Omega\ cm^{-1}$, dielectric strength of 14 $kV\ mm^{-1}$), the sputtering system uses rf power and argon ion plasma to deposit the films. On the other hand, the latter and more recent reactive magnetron sputtering technique for deposition of aluminum nitride films uses an elemental aluminum target with the plasma consisting of nitrogen and argon ions. This reactive magnetron sputtering technique is based upon a low free energy of formation of aluminum nitride (ΔH at 298 K$=-76.1$ kcal/mol, ΔS at 298 K$=4.8$ kcal/deg mol) when aluminum ions sputtered in argon ion plasma react with the nitrogen ions also present in the plasma. In addition to the high cost of the power source and matching circuit in the rf system, the deposition rate of AlN

is also found to be very low. These disadvantages are overcome in the pulsed direct current (dc) power system used in the reactive magnetron sputtering of aluminum target. The formation of an insulating film by reaction at the target surface and charge build up from ion bombardment give rise to electric fields that can easily exceed the dielectric strength of AlN film at the target surface and arc formation. Arcing is avoided in rf sputtering wherein electrons are attracted to the target surface on the positive peak of every cycle and discharge any insulating regions formed. Depending on the dielectric constant of the reaction product and the current density of the arriving gas, the charged layers can be discharged at relatively low frequencies. The power supply that has been used in the present reactive magnetron sputtering of AlN generates a series of 75 kHz dc pulses modulated with 2.5 kHz frequency. In pulsed dc magnetron sputtering, an electron trap is formed over the cathode surface and an intense plasma is generated. The ions from the plasma are drawn to the target surface and change the potential that also causes the electrons to leak from the plasma. These electrons are attracted to the anode of the system or the chamber and generate a return current to the power supply. The surface of the chamber is also coated with the insulating AlN film providing no return path for the electrons to the power supply that raises the impedance of the load and an attendant increase in voltage with the formation of a more diffusive or even extinguishing plasma. This problem is avoided by cleaning the chamber frequently after deposition of insulating film such as AlN. It has been well established that deposition rate of AlN is reduced with increase in frequency above 30 kHz. However, the deposition rate is 80% higher than at rf frequency of 13.56 MHz. The quality of the films has been found to be independent of the frequency and stoichiometric films can be obtained using 75 kHz pulsed dc source. Large area deposition of aluminum nitride (up to 8 inch diameter wafers) is considered to be an advantage in magnetron sputtering method.

We have deposited AlN films by pulsed dc reactive magnetron sputtering using ultrahigh purity argon and nitrogen gas mixture at different ratios of partial pressures of argon and nitrogen and an aluminum target of 99.999% purity. The predeposition vacuum was maintained at $<5\times10^{-7}$ Torr. Si(111) substrates were cleaned to remove the surface oxide layer using a 5% HF solution. The substrates for deposition were heated radiatively and the temperature was measured by a thermocouple pressed directly on to a silicon dummy wafer specimen kept close to the substrate. The substrate temperature was varied between 300 and 750 °C and the circulating sputtering power is optimized between 0.5 and 1.25 kW. The deposition time of the films was varied from 30 to 45 min after initial cleaning of the aluminum target for 5 min and predeposition of AlN for an additional 3 min. A shutter was used to cover the silicon substrate during cleaning and predeposition periods. In RMS, the effective power accounts for the ions in the plasma whereas the circulating power is that applied to generate the plasma. The effective power during cleaning of aluminum target was found to be 1.20 kW and the circulating power approximately a quarter of the effective power. On the other hand, the deposition of aluminum nitride is characterized by the observed effective power of 0.55 kW compared to the circulating power of 1.2 kW that is approximately twice that of the effective power. This difference in the magnitudes of effective and circulating power during sputtering of aluminum on one hand with argon ion plasma and with argon and nitrogen ion plasma on the other is explained by the metallic and insulating nature of the deposited films, respectively. The partial pressure of argon was optimized at 0.6 mTorr with that of nitrogen kept at 0.4 mTorr so that the total sputtering pressure was 1 mTorr. The thickness of the AlN films deposited for 30 minutes with sputtering current of 2.0 A and sputtering pressure of 1 mTorr was measured using a profilameter and found to be close to 300 nm.

B. Pulsed laser deposition

Pulsed laser deposition is a technique that is very useful for the deposition of compound films such as oxides, nitrides and carbides of different metals including elemental (single element) films. As mentioned earlier, PLD lends itself to low-temperature processing because the average energy of species in the laser evaporated plume is considerably higher ($\sim$10 eV) than the thermal evaporation energy ($\sim$0.1 eV) and therefore the fraction of ionic species in the laser generated plasma is higher than in any other technique.[13] The additional energy of atomic and molecular species during laser ablation improves the mobility and results in better crystallization at lower temperatures compared to the films deposited by equilibrium evaporation methods. Thus, the substrate temperature is an important factor in achieving high quality crystalline films. The high energy of the supersaturated vapor in the pulsed laser generated plasma ($\sim10^5$ J/mol) attained in a very short time and quenching on the substrate classifies PLD a highly nonequilibrium nature suitable for the formation of compounds. A very important feature of PLD is that it preserves nitrogen or oxygen stoichiometry of the target in deposited films. The laser ablation of aluminum target in nitrogen plasma may not be suitable for the formation of a good quality nitride film as aluminum is known to eject a high fraction of aluminum particulates in PLD that can not readily and completely react to form stoichiometric nitride. We have, therefore, employed a compound AlN target to grow films by PLD. The AlN compound target used in PLD often contains small quantities of binder material that is incorporated into the deposited films as impurities. In certain cases, although not in the present, this unfavorable situation may be turned to an advantage by intentional incorporation of certain atomic species to dope the deposited films. The sintered polycrystalline AlN target gives out oxygen due to desorption from heating of the target. Therefore, we have cleaned the target surface *in situ* prior to deposition of AlN films while keeping the substrate covered with a shutter.

An efficient source of atomic or ionic (N^+) nitrogen is a key to the formation of high quality epitaxial nitride films

from the elemental target. It is well known that nitrogen molecule is very stable (bond dissociation energy ~9.7 eV) and generates only a very small fraction (≤10%) of ionized atomic species. Therefore, other suitable sources of atomic or ionic nitrogen are essential to form high quality aluminum nitride films when prepared from an elemental target. In techniques such as reactive magnetron sputtering, plasma of nitrogen is generated. Formation of aluminum nitride by PLD from an aluminum target in the presence of nitrogen ions generated from a Kauffman ion source has been found to be incomplete leaving large quantities of aluminum. The lack of atomic or ionic nitrogen is overcome in PLD by laser ablation of an aluminum nitride target with the optimum laser energy density so that AlN in molecular form may be generated near the substrate surface. Another drawback associated with the growth of AlN films by any technique is the incorporation of oxygen in the films because of the high affinity of aluminum to oxygen. Deposition of AlN under ultrahigh vacuum conditions ($<10^{-7}$ Torr) is essential to reduce the oxygen levels in the films obtained by PLD.

Deposition of aluminum nitride was performed using pulsed excimer (KrF) laser ($\lambda = 248$ nm, pulse duration $t = 25$ ns). The pulsed laser beam was focused on an AlN target placed in a chamber evacuated to $\sim 10^{-8}$ Torr predeposition vacuum. The stoichiometric hot pressed AlN target was ablated at an energy density ranging from 3 to 10 J/cm^2 with pulse repetition rate of 10 Hz for 30 min. The substrate, kept 3.5 cm away from the target, was heated radiatively to keep the substrate at the desired temperature. The deposition was carried out at different temperatures in the range of 300–750 °C. Nitrogen gas of ultrahigh purity was introduced into the PLD chamber at partial pressures ranging from 10^{-7} to 10^{-4} Torr during deposition. The thickness of the AlN films was measured using a profilameter and found to be close to 300 nm for a deposition period of 30 min. The films used for wear test were deposited at the substrate temperature of 600 °C for longer time to attain a thickness of 1 μm by either PLD or RMS techniques. The larger thickness of the film for wear test was desired to observe the wear of the film and that of the interfacial region.

The films deposited by RMS and PLD were characterized using x-ray diffraction (XRD) and transmission electron microscopy (TEM) with high resolution facility for determination of epitaxial growth relation, grain size, crystallinity and defect structure of the films. Raman spectroscopy and Fourier transform infrared spectroscopy (FTIR) were used to determine the crystalline quality and residual stresses present in the films. The stoichiometry and composition of the films, in terms of the relative levels of impurities of oxygen and silicon, were determined by secondary ion mass spectrometry (SIMS). We have also evaluated the adhesion strength by a scratch test and wear resistance by use of a dimpling machine. The results of the various characterization techniques used to determine the quality of the films deposited by RMS and PLD are presented below.

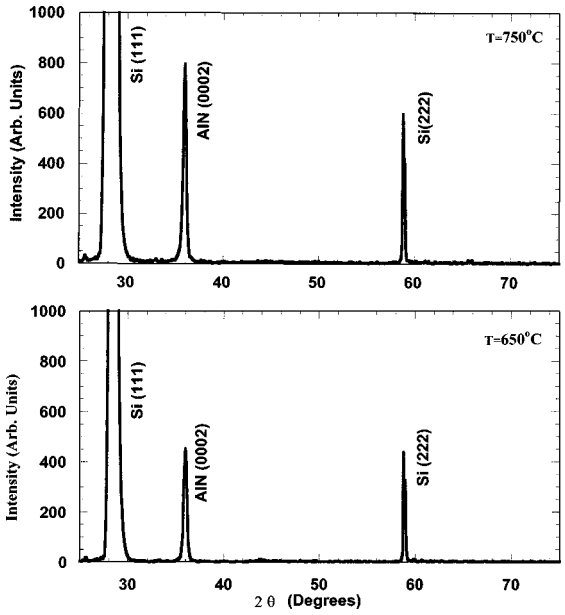

FIG. 1. X-ray scans obtained from AlN films deposited by RMS at 650 and 750 °C.

III. RESULTS

A. X-ray diffraction

The XRD of thin films was carried out using a Rigaku diffractometer with a Cu $K\alpha$ radiation operating at 30 kV voltage and 20 mA current. The substrate was initially aligned for Si(111) and normal θ-2θ scan was recorded in the $2\theta = 15° - 100°$ range. Figure 1 shows θ-2θ scans obtained on films deposited by RMS at 650 and 750 °C. The scans for the films deposited at a temperature of 500 °C and below showed polycrystalline structure with strong texture that is revealed by the presence of stronger (0002) reflection of aluminum nitride compared to the weaker (1010) and (1011) reflections. The films deposited at 650 and 750 °C showed only the (0002) reflection, as shown in Fig. 1. The alignment of the Si(111) peak with that of AlN(0002) improved indicating that the basal plane (0001) of AlN is parallel to the (111) plane of silicon. The preferred growth direction of hexagonal AlN is normal to the basal plane provided the temperature is sufficiently high. The x-ray rocking curve for the films deposited at 650 °C and above was very broad indicating the films were textured and in-plane alignment was not very good. The broadening of the diffraction line was measured by the full width at half maximum (FWHM) of intensity. The FWHM was 0.40° for deposition temperature of 650 °C and above whereas it increased to 0.50° at 500 °C. At temperatures below 500 °C, the peaks were very broad. It was further confirmed by results from Raman spectroscopy, presented below, that the films were partially amorphous. Using the broadening of the x-ray peak in the form $B = 0.9\lambda/d \cos\theta$, where B is the FWHM of the peak, λ is the wavelength of the incident radiation (Cu $K\alpha = 0.154$ nm), d is the crystalline diameter, θ is the diffraction angle for the

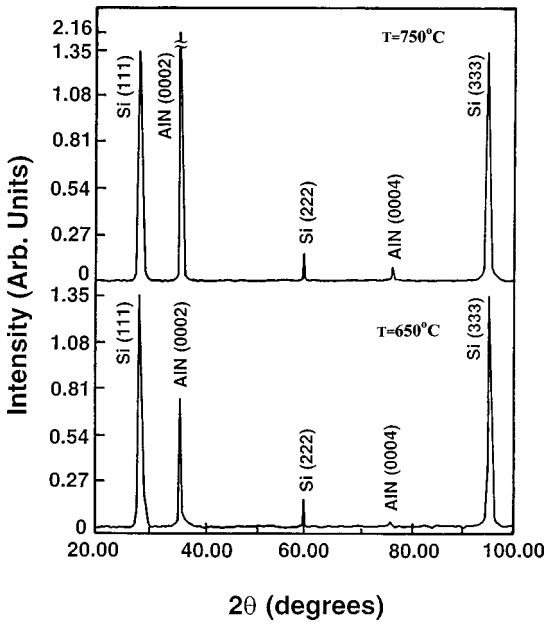

FIG. 2. X-ray scans obtained from AlN films deposited by PLD at 650 and 750 °C.

AlN(0002) reflection, the crystallite sizes decreased from 25 to 18 nm when substrate deposition temperature was reduced from 750 to 500 °C.

Figure 2 shows the x-ray scans of AlN films deposited on Si(111) by PLD at two different temperatures. The films exhibited reflections from the (0002) and (0004) planes of AlN aligned with Si(111) reflection. The width of the rocking curves was quite broad indicating poor inplane alignment of the grains. The FWHM measured from the films deposited at 550, 650, and 750 °C, showed a decrease from 0.45° to 0.36° and 0.28°. The crystallite size calculated from the above formula of x-ray line broadening increased from 18 to 30 nm when the substrate temperature increased from 550 to 750 °C. These results of peak broadening again indicate that the sizes of the crystallites in the films deposited by PLD were comparable to those in films deposited by RMS. The intensity and the FWHM values of the AlN(0002) peaks from films deposited by PLD were comparable to that of the peaks obtained from films deposited by RMS. A decrease in the intensity of the AlN(0002) reflection by a factor of 3 and a corresponding increase in the FWHM in the films deposited for the same time by PLD at higher partial pressures of nitrogen of up to 10^{-4} Torr showed that the crystalline quality is reduced. In addition, particulate formation in the AlN films was observed at higher partial pressures of nitrogen.[4]

B. Transmission electron microscopy

Figure 3(a) is a cross-sectional high resolution lattice image of AlN films on Si(111) deposited at 500 °C by RMS. A disordered region is observed at the interface between the AlN film and the silicon (111) substrate. We believe this disordered phase is either silicon oxide or silicon nitride layer formed by reaction of nitrogen plasma with the silicon substrate in the predeposition stage of film deposition. Figure

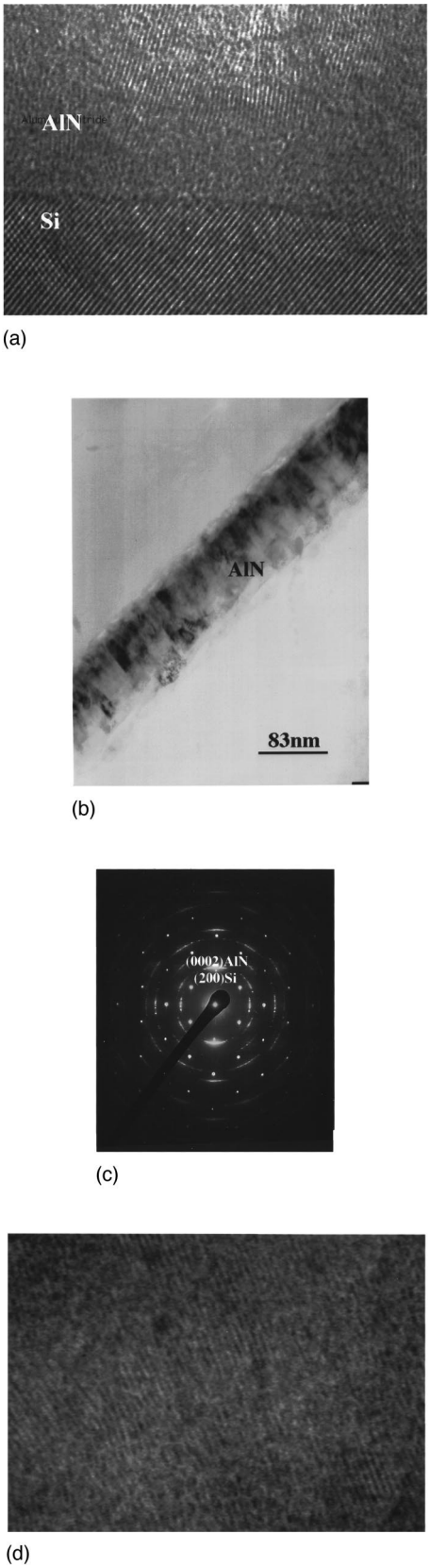

FIG. 3. (a) Cross-sectional high resolution TEM image of AlN film on Si(111) deposited by RMS at 500 °C. (b) Bright-field TEM image of the AlN film on Si(111) substrate deposited by RMS at 500 °C. (c) Selected area diffraction pattern of the AlN film on Si(111) substrate shown in (b). (d) Plan-view high resolution TEM image of the AlN film on Si(111) substrate deposited by RMS at 500 °C.

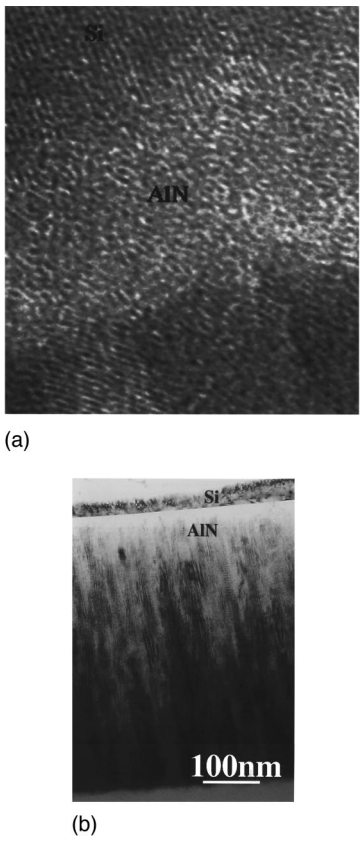

FIG. 4. (a) Cross-sectional high resolution TEM image of AlN film on Si(111) deposited by RMS at 600 °C. (b) Bright-field TEM image of the AlN film on Si(111) substrate deposited by RMS at 600 °C.

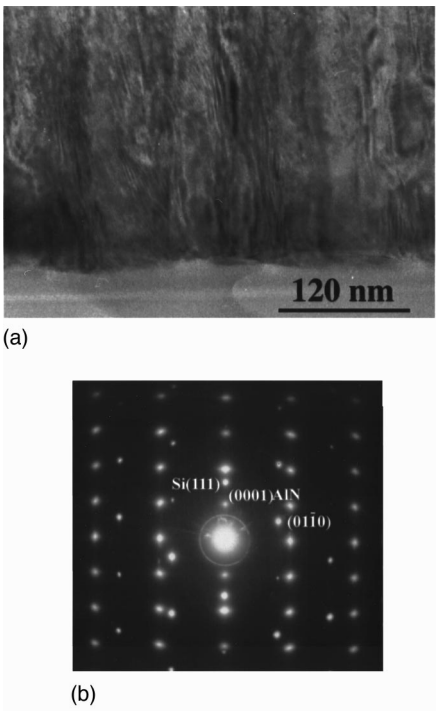

FIG. 5. (a) Diffraction pattern of the AlN film on Si(111) substrate deposited by PLD at 750 °C. (b) Cross-sectional bright field TEM image of AlN film on Si(111) deposited by PLD at 750 °C.

3(b) shows the bright-field (BF) image of the AlN layer with the grain boundaries located normal to the interface. The diffraction pattern obtained from the film with the presence of Debye arcs centered around the diffraction spots, as shown in Fig. 3(c), confirms that the growth of the films is highly textured. The average grain size measured from Fig. 3(b) is close to 20 nm that matches well with the grain size estimated from the x-ray line broadening of the AlN(0002) reflections from the same samples. Figure 3(d) is the plan-view, high resolution image of AlN film deposited at 500 °C. The average grain size estimated from this electron micrograph is close to 20 nm that again agrees with the results of XRD and cross-sectional TEM results. Figure 4(a) shows the high resolution lattice image of the AlN film deposited at a substrate temperature of 600 °C by RMS. An interfacial layer that is not identified in composition because of the very small dimensions is seen at the interface in this image. Thus, the possibility of reaction of nitrogen plasma or AlN with the substrate should be considered. Figure 4(b) is a bright-field image of the AlN film with the Si(111) substrate. The average grain size estimated from this micrograph is ~35 nm that is slightly larger than the estimated value by line broadening analysis of XRD, AlN(0002) peaks. The films deposited by PLD were also found to be highly textured at substrate temperatures of 550, 650 and 750 °C. Figure 5(a) is the electron diffraction pattern and Fig. 5(b) the corresponding cross-section high resolution TEM image of a region from the AlN/Si interface. The observed epitaxial relationship is given by AlN(0002)[$\bar{1}$120]‖Si(111)[110].[4–6,9–12]

C. Raman spectroscopy

The films deposited either by PLD or RMS were characterized by Raman spectroscopy using a Spex 1704- 1 m spectrometer with a holographic notch filter to reject the stray elastically scattered laser light. The excitation wave length was 514.5 nm green light from the Ar^+ ion laser and was chosen to be incident at a low angle of 15°–20° to the plane of the AlN film. The scattered light was collected into the spectrometer slit of width 200 μm. The spectrum was collected in the photon counting mode with count time of 60 s at each value of wavelength incremented in 0.05 nm steps. The spectrum was collected from a starting wavelength of 520 nm to a final wavelength of 545 nm to observe the most important peaks associated with AlN. Table I shows the characteristic Raman peaks associated with amorphous and crystalline hexagonal AlN and the observed values in the range of our investigation.[14–18] Raman scattering from AlN films is not very strong and therefore long count times were used.

Raman spectrum observed from AlN films deposited by RMS at 650 °C and above is shown in Fig. 6(a) and that from the films deposited at 500 °C is shown in Fig. 6(b). The film deposited at 650 °C exhibited all the major peaks associated with crystalline AlN film, shown in Table I, but the peaks were broad and shifted from the characteristic values by few wave numbers. We associate the broadening of the

TABLE I. Characteristic phonon modes and observed Raman shifts in AlN films deposited by reactive magnetron sputtering and pulsed laser deposition.

Stokes shift (cm^{-1})		Phonon Mode		
Crystalline[a)]	Observed	Amorphous[b]		Observed
610,659	615-620, 650-670	514		A_1(TO) (*ir* active)
655	650-670			E_2 (*ir* inactive)
614,667	615-620, 650-670			E_1(TO) (*ir* active)
895,910	895	788,825	765-790	E_1(LO) (*ir* active)
888	885	650,746	650–670,746	A_1(LO) (*ir* active)

[a]Refs. 14–17.
[b]Ref. 15.

peaks to the smaller crystallite size and the shift from the characteristic value to the compressive residual stress present in the film. The Raman spectrum obtained from the AlN film deposited by PLD at a substrate temperature of 750 °C is shown in Fig. 7. Similar to the Raman spectrum observed from AlN films deposited by RMS, all the peaks associated with crystalline AlN are observed in Fig. 7. In addition, Raman peaks were also observed at 745, 785 and 825 cm^{-1} in films deposited at lower substrate temperatures by either RMS or PLD. These peaks, as shown in Table I, are associated with the amorphous phase of AlN.[15] The intensity of these peaks relative to that of the crystalline peaks is found to increase for films deposited at lower substrate temperature. We believe the fraction of amorphous phase increased at lower temperatures and as a result the Raman peaks associated with the amorphous phase became prominent.

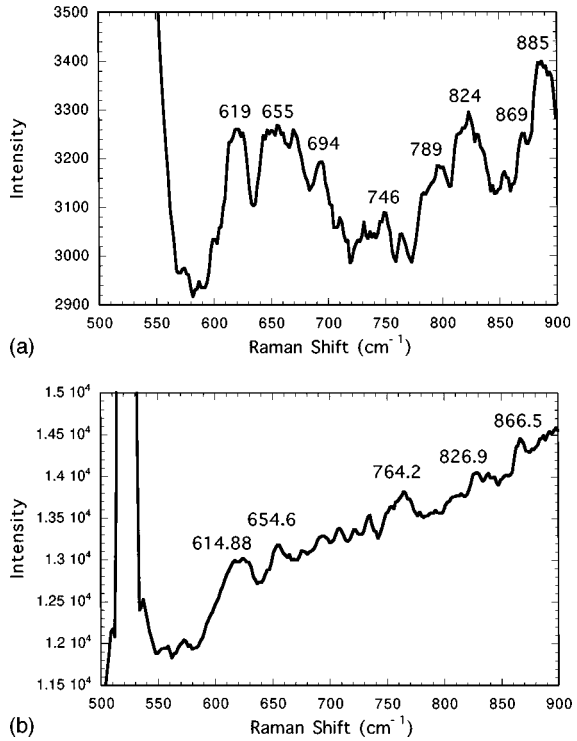

FIG. 6. (a) Raman spectrum from AlN film on Si(111) substrate deposited by RMS at 650 °C. (b) Raman spectrum from AlN film on Si(111) substrate deposited by RMS at 500 °C.

D. Fourier transform IR spectroscopy

We have also characterized the AlN films deposited by either PLD or RMS using FTIR spectroscopy. FTIR is a complementary technique to investigate characteristic vibrational frequencies of the lattice that are not Raman active. The characteristic value of 667 cm^{-1} in absorption is known to arise from either A_1 (TO) or E_1 (TO) phonon modes of AlN that are IR active. The A_1 and E_1 (LO and TO) phonon modes of AlN are known to be both IR and Raman active and these are the Brillouin zone center ($k=0$) phonons. The A_1 and E_1 (LO) phonons are shown to appear near 910 cm^{-1} and E_2 mode at 665 cm^{-1} that alone is IR inactive, as shown in Table I. The spectra were recorded in the transmission mode on a Galaxy series FTIR 5000 instrument. The background subtraction was performed by recording a spectrum from a Si substrate of the same orientation and thickness. The observed peak from films deposited by RMS shifted from the characteristic value of 667 cm^{-1} to a value between 670 and 674 cm^{-1}. Figure 8(a) shows FTIR spectrum of AlN films deposited by RMS at 500 and 600 °C with a peak near 670 cm^{-1}. The spectrum for films deposited at and above 600 °C was not different. We have chosen to report the results for the films deposited at 600 °C to illustrate the nature of stresses present in the films, and in particular, to compare with the films deposited by PLD at the same temperature. Figure 8(b) shows the FTIR spectrum from the AlN films deposited by PLD at 600 and 750 °C. The films deposited by PLD at a substrate temperature of 750 °C exhibited a peak

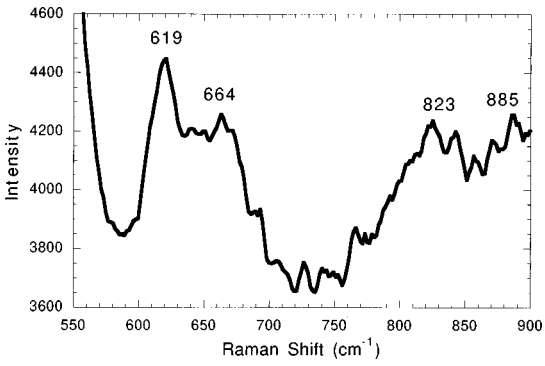

FIG. 7. Raman spectrum from AlN film on Si(111) substrate deposited by PLD at 750 °C.

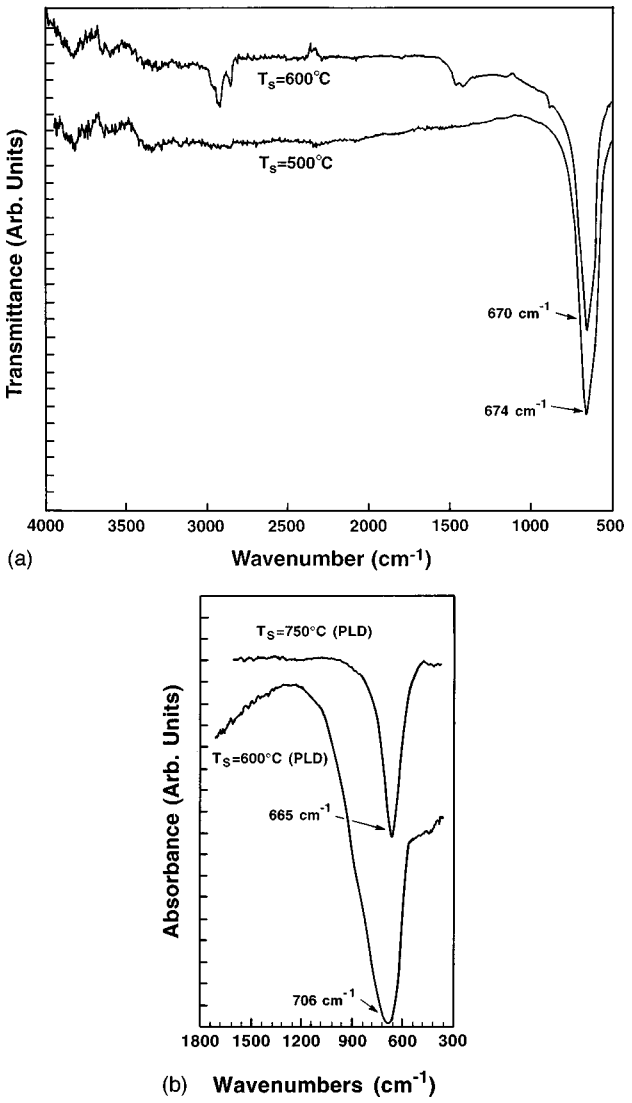

FIG. 8. (a) FTIR spectrum of AlN film on Si(111) substrate deposited by RMS at 500 and 600 °C. (b) FTIR spectrum of AlN film on Si(111) substrate deposited by PLD at 600 and 750 °C.

near 665 cm^{-1}. However, the films deposited at a lower temperature of 600 °C showed a broader peak centered around 706 cm^{-1}. We believe this large shift in the IR absorption peak arises from the residual stress present in the films deposited by PLD at 600 °C and below. Hydrostatic applied stress in the range of 5–10 GPa, resulting in a lattice strain of the order of 0.0075 to 0.015, has been found to give rise to a shift in the A_1 and E_1 (TO) modes of AlN to a higher value, up to about 700–710 cm^{-1}, respectively. The presence of compressive stress in the films deposited by PLD at lower substrate temperature can arise from several reasons. The nonequilibrium nature of PLD leading to quenching of deposited species from the laser generated plume with high energy (10–1000 eV) on the substrate maintained at lower temperature (600 °C) could be one of the factors. When the substrate temperature is high, the adatom mobility is high and therefore better crystalline quality is reached and the stresses are relaxed. Secondly, the oxygen concentration in the films deposited by PLD at lower substrate temperature (600 °C) is found to be high, as shown by SIMS analysis presented below. Higher residual stress is expected as a result of higher oxygen incorporation and lower substrate temperature during deposition. Apparently, this large compressive stress present in the AlN films deposited by PLD is responsible for poor adhesion of the films to the substrate.

E. Secondary ion mass spectrometry

Oxygen impurities present in AlN in the films may create mid-gap states[19] and also may lower the thermal conductivity so that it becomes less attractive for most applications. In order to compare the oxygen levels present in the films deposited by both techniques, SIMS analysis was carried out using Cameca IMS-6F with Cs^+ ion beam. In addition, silicon diffusion into the AlN films deposited at a higher substrate temperature is an important consideration in their use for electronic applications such as formation of dielectric films. Figures 9(a) and 9(b) show the SIMS profiles obtained from the films deposited by RMS and PLD at a substrate temperature of 600 °C, respectively. Specifically, SIMS analysis on a film deposited at 600 °C was carried out since the same film was used in the wear test. In addition, the residual stress in the film deposited at 600 °C was found to be much higher as revealed by a large shift in the peak in the FTIR spectrum. The results of SIMS analysis, obtained for comparison purpose, clearly indicate that the oxygen level is relatively higher in the films deposited by PLD compared to those in films deposited by RMS. Since the SIMS results are more sensitive,[20] by at least a factor of 12 to oxygen than to aluminum, we believe it is difficult to make a quantitative estimate, specifically in the absence of a known standard. However, comparison of oxygen to aluminum or oxygen to AlN and that of aluminum to AlN signals clearly illustrates that higher oxygen impurities are present in AlN films deposited by PLD. The high affinity of aluminum to oxygen present in the chamber is responsible for oxygen incorporation into these films. Unless the AlN films are deposited by PLD at ultrahigh vacuum levels ($<10^{-8}$ Torr), incorporation of oxygen can not be reduced to less than 1 at. %.[14] The AlN films, in the present work, have been deposited by PLD with a predeposition vacuum better than 4×10^{-7} Torr and hence the higher level of oxygen impurities may have originated from the target. Because the polycrystalline targets used in PLD are prepared by sintering at higher temperatures to achieve high density, oxygen impurities may be incorporated during the processing steps. We believe oxygen in the target is responsible for incorporation at higher levels in AlN films deposited by PLD. On the other hand, a high purity (99.999%) aluminum target has been sputtered by Ar^+ ions for the first five minutes prior to the deposition of AlN while the substrate is masked by a shutter in RMS. This initial cleaning procedure of the aluminum target may be responsible for removal of the oxygen present in the chamber since aluminum has high affinity for oxygen. We believe the sputtering of aluminum ions is responsible for the gettering of oxygen in the vacuum system and thereby produces the rela-

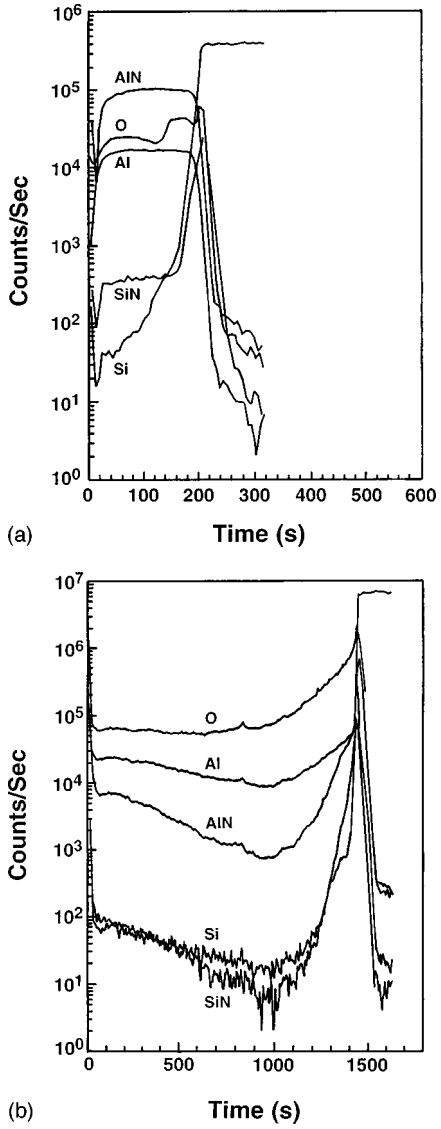

FIG. 9. (a) SIMS depth profiles of aluminum, oxygen and nitrogen in Si–N and Al–N bonds in AlN film on Si(111) substrate deposited by RMS at 600 °C. (b) SIMS depth profiles of aluminum, oxygen and nitrogen in Si–N and Al–N bonds in AlN film on Si(111) substrate deposited by PLD at 600 °C.

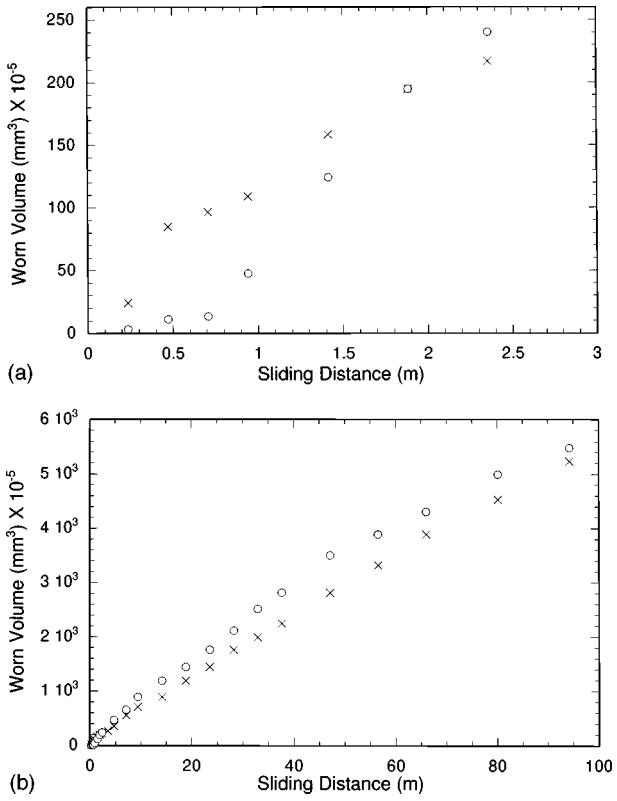

FIG. 10. (a) Wear volume determined from microscopic wear test of AlN films on Si(111) substrate. The full circles represent AlN film deposited by PLD at 600 °C and the crosses represent the AlN film deposited by RMS at 600 °C. (b) Same as (a) except the results are shown for longer time of the wear test.

tively lower level of oxygen found in the AlN films deposited by RMS. Silicon and Si–N mass spectra were also obtained to determine if silicon diffusion into AlN films is high. Both Si and Si–N were also found in smaller quantities in the films deposited by both of these techniques, as shown in the SIMS results presented in Figs. 9(a) and 9(b). Silicon diffusion along grain boundaries during deposition at 600 °C or above is expected in films deposited by both techniques. The concentration of Si–N bonds appears to be higher in the films deposited by RMS than in films deposited by PLD, as seen in Figs. 9(a) and 9(b). Reaction of nitrogen with Si substrate surface is expected in the initial stages of deposition when nitrogen plasma is generated in the RMS process. Therefore, the thin reaction layer is considered to be an amorphous film of silicon nitride formed at lower substrate temperature. Diffusion of silicon in AlN films deposited by PLD is also higher as seen by the silicon levels in the range of 10^1-10^2 in the SIMS results.

F. Wear and scratch tests

Wear tests were performed with a dimpling machine usually used for a TEM sample preparation. The dimple grinding machine consists of a circular wheel that rotates at constant speed and causes wear in contact with the specimen surface. Different particulate suspensions may be employed as an abrasive. In the present wear tests, alumina suspension of size 0.5 μm was used. This microscopic abrasive wear test has been found appropriate in the characterization of the wear resistance of very thin films deposited in our laboratory. The wear volume was calculated from the diameter and depth of the spherical wear impression made by the circular wheel. As mentioned earlier, the thickness of AlN film used in the wear tests was chosen to be larger and close to 1 μm to provide enough depth for wear. Figure 10(b) describes the wear performance of the two AlN films deposited by PLD and RMS for the complete duration of the wear test, while the initial stages of the wear performance are plotted in Fig. 10(a). These results illustrate better wear resistance of films deposited by PLD in the initial stages of the wear test compared to those deposited by RMS. The better wear resistance of the films in the initial stages may be attributed to a higher

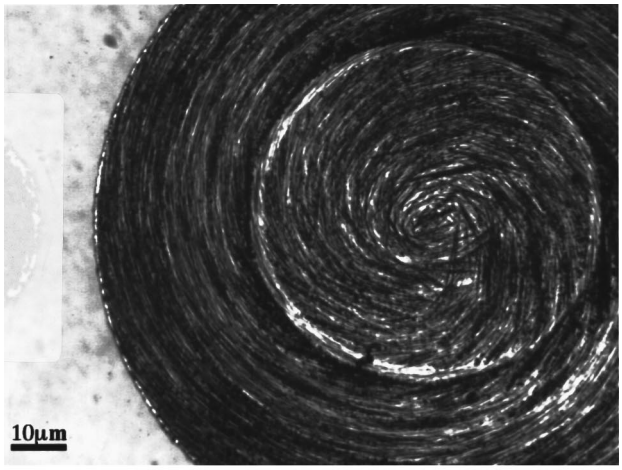

(a)

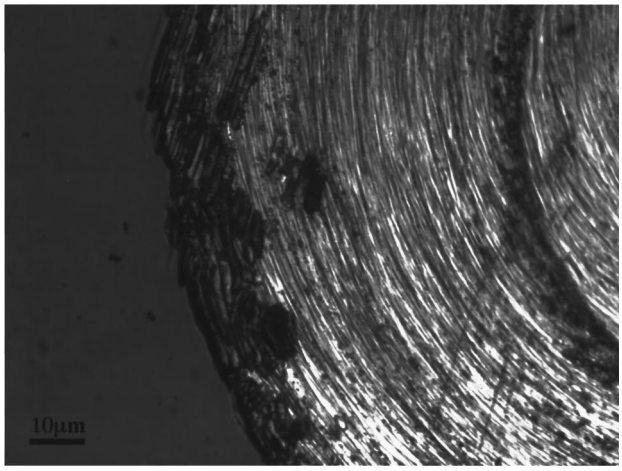

(b)

FIG. 11. (a) Wear surfaces observed after microscopic wear test using dimple grinder of AlN films on Si(111) substrate deposited by RMS at 600 °C. (b) Wear surfaces observed after microscopic wear test using dimple grinder of AlN films on Si(111) substrate deposited by PLD at 600 °C.

hardness of the PLD deposited films. PLD films exhibit higher hardness because of the larger residual compressive stresses present. In the initial stages of the wear test using the dimpling machine, the circular wheel essentially slides on the film only and therefore the interface of the substrate-film composite is not in contact with the wheel. In the latter stages of the wear test, however, a crater is already formed in the film and therefore only the peripheral part of wheel slides on the film but the major area of contact remains on the substrate. In this second stage of wear, adhesion of the film to the substrate becomes an important factor in the wear resistance offered by the composite. When the film exhibits poor adhesion, delamination of the film from the substrate has been found during the second stage of the wear test. Figures 11(b) and 11(a) are the optical micrographs of the craters formed on the films deposited by PLD and RMS, respectively. The edges of the crater are smooth in case of films deposited by RMS, whereas, films deposited by PLD exhibit irregular edges as a result of delamination of the small regions of the films from the edges. As pointed out already, this delamination of the film in the second stage of wear test is suggestive of the lower adhesion of the PLD films to the substrate. Lower adhesion strength of the film to the silicon substrate arises from the presence of large residual compressive stress in the films deposited by PLD at lower substrate deposition temperature (600 °C), a result substantiated by large peak shift in FTIR spectrum and higher oxygen level in the SIMS analysis. The wear performance of AlN films deposited by RMS is observed to be better in the second stage, a result expected from the better adhesion strength with the substrate. Therefore, the compressive stress-induced poor adhesion of the AlN film deposited by PLD is responsible for the poor wear resistance also.

Coefficient of friction of the AlN films at room temperature ambient conditions was determined using a scratch test. In this test, tangential load required to slide a sharp diamond indenter was determined for different magnitudes of applied normal load. Load applied normal to the surface increased up to 20 g with the tangential load in the range 0–11 g. The coefficient of friction of AlN films deposited by PLD was higher (0.6) compared to that of films deposited by RMS (0.4). The higher coefficient of friction is associated with the presence of particulates that are known to form in films deposited by PLD. We have also observed that higher tangential loads were applied for the same normal load before the AlN films deposited by PLD could be scratched to create a wear track on the surface compared to the films deposited by RMS. Figure 12(a) is an optical micrograph of the wear track on the AlN film deposited by PLD using a normal load of 10 g and the tangential load of 5 g. The film is found to delaminate at certain points along the wear track. The delamination of the PLD film again illustrates the poor adhesion to the silicon substrate. Figure 12(b) is an optical micrograph of the wear track on the AlN film deposited by RMS under the same normal load of 10 g but with the tangential load of 3 g. The diamond tip is observed to have made a deeper impression with delamination of the film along the complete length of the wear track. Similar differences in the behavior of AlN films deposited by PLD and RMS were observed in the scratch test made at different applied normal loads. As mentioned already, the residual compressive stress in the film deposited by PLD at substrate deposition temperature of 600 °C was higher than the stress in the films deposited by RMS, thus, giving rise to higher hardness and also improved wear resistance. A higher coefficient of friction for the films deposited by PLD is related to the presence of particulates and a nonuniform surface.

IV. DISCUSSION

Aluminum nitride films deposited on silicon (111) substrate by PLD and RMS in the temperature range of 300–750 °C and predeposition vacuum of 2×10^{-7} Torr were found to be textured with crystallite size in the range of 20–40 nm. The epitaxial growth behavior of the AlN films followed the previously observed relationship given by

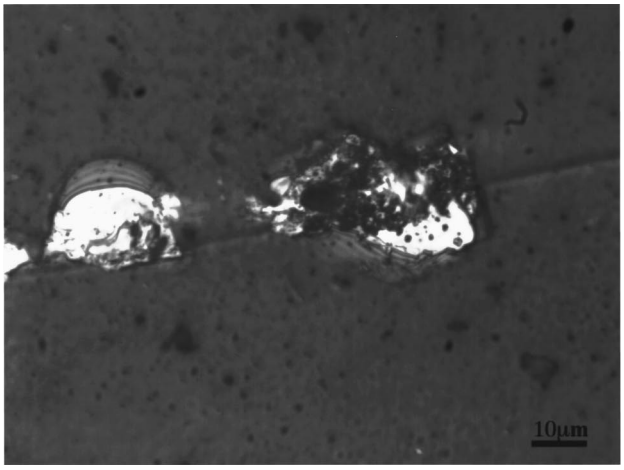

(a)

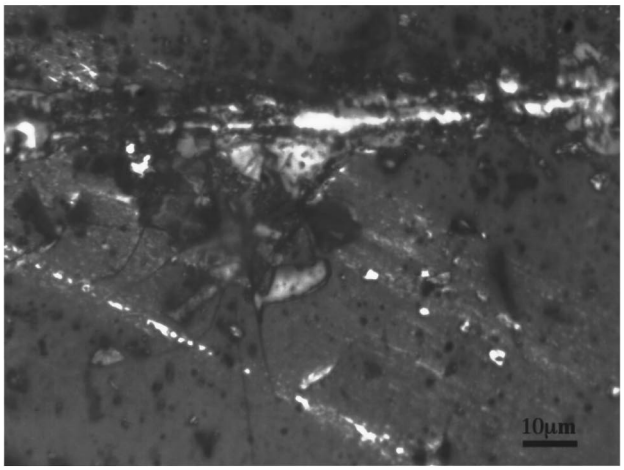

(b)

FIG. 12. (a) Optical micrograph of the wear track obtained after scratch test of the AlN film on Si(111) substrate deposited by PLD at 600 °C. (b) Optical micrograph of the wear track obtained after scratch test of the AlN film on Si(111) substrate deposited by RMS at 600 °C.

$AlN(0002)[1\bar{1}20]\|Si(111)[\bar{1}10]$. The domain mismatch between four atomic spacings along Si [110] and five of AlN [1120] is evaluated to give a compressive strain of −0.01278 in the film. Therefore, in the initial stages of growth and before relaxation of the strain takes place, the film is subjected to residual compressive stress, a result also previously observed by in-situ stress measurements of wafer curvature.[11,12] These compressive stresses were associated by the previous authors[11,12] with surface stress effect. Although Raman spectroscopy has been carried out after deposition, residual stress evaluation using the peak shift measurements, in comparison with the results of wafer curvature measurements, was not presented.[11,12] Furthermore, the wafer curvature measurements indicate that the magnitude of compressive stresses increase with thickness for deposition at room temperature whereas these are reduced with thickness for deposition carried out 800 °C. The partial reduction in compressive stresses at 800 °C is attributed to grain boundary stress relaxation or surface relaxation mechanisms.[11,12]

TABLE II. Residual stress calculated from the observed values of domain mismatch strain, thermal strain, Raman and FTIR peak shifts.

Film	$C(0001)$ (GPa)	Domain (GPa)	Thermal (GPa)	Raman (GPa)	FTIR (GPa)
AlN(RMS) at 600 °C	509.6	−6.6	0.60	−7.7 to −8.4	−5.4
AlN(PLD) at 750 °C	509.6	−6.6	0.80	−1.0 to −2.0	0
AlN(PLD) at 600 °C	509.6	−6.6	0.60	⋯	−29.8

Residual stresses are known to arise from three factors: (1) intrinsic stresses due to defects such as vacancies, dislocations, grain boundaries, and impurities, (2) lattice or domain mismatch stresses, and (3) thermal stresses resulting from differences in thermal expansion coefficients. There is contribution to residual stresses from different components of strain that include domain or lattice mismatch, thermal and defect induced strains. The resultant lattice strains evaluated from Raman and FTIR peak shifts can be used to calculate the magnitude of residual stress using[12]

$$\sigma = C\epsilon = (c_{11} + c_{12} - 2c_{13}^2/c_{33})\epsilon,$$

where ϵ is the in-plane invariant strain and C is the elastic modulus evaluated from the elastic constants c_{ij} of AlN.[21–24] The shortened subscript notation of the elastic constants c_{ijkl} is used in the above equation. The results of these calculations are given in Table II where in addition to the domain mismatch and thermal strain, lattice strains determined from Raman or FTIR peak shift are used in the form $\epsilon = -\Delta\omega/\omega$, where $\Delta\omega$ is the shift to higher value compared to the unstressed value of ω in wave numbers (cm^{-1}). The net result of residual stress present in the film at room temperature determined from Raman or FTIR peak shift is shown in Table II.

From previous discussion, the lattice or domain mismatch stresses are compressive that cannot be relaxed at room temperature since formation of glide dislocations is prevented by the high lattice frictional stress in AlN. Diffusional motion of the atoms is also restricted at room temperature. However, we expect the stresses to be relaxed at least partially for films deposited at 600 °C. The intrinsic stresses can either be compressive or tensile. Presence of excess vacancies in the lattice, for example, nitrogen vacancies is responsible for tensile stresses. On the other hand, excess nitrogen or oxygen ions introduced as interstitials can be responsible for compressive stresses. These compressive stresses can only be relieved by diffusion of the oxygen ions from the lattice that does not take place because of the high affinity of oxygen to aluminum. AlN films deposited at high sputtering pressure of argon and nitrogen are found to be deficient in nitrogen and hence the residual stresses are tensile.[10] Therefore, domain mismatch stresses start to be compressive in the initial stages of deposition and change to become tensile with increase in thickness when the compressive stresses are overcome. However, if oxygen levels incorporated into the film are suffi-

ciently high, residual compressive stresses increase and cannot be annealed out completely. The thermal strain in AlN film deposited at higher temperature is given by $(\alpha_{AlN} - \alpha_{Si})\Delta T$, where α's are the respective linear thermal expansion coefficients and ΔT is the difference between deposition temperature and room temperature. Using $\alpha_{AlN} = 5.2 \times 10^{-6}$/K and $\alpha_{Si} = 3.2 \times 10^{-6}$/K and $\Delta T = 600$ °C, the magnitude of tensile residual strain in the film is 0.0012 that is much smaller than the domain mismatch strain that is compressive. Therefore, we do not expect the net residual stresses to become tensile unless the domain mismatch stresses are relaxed completely at the deposition temperature and tensile thermal stresses remain upon cooling.

The peak shifts measured by Raman and FTIR spectroscopy from the AlN films deposited by PLD and RMS in the present work illustrate the presence of only compressive stresses, as shown in Table II. These compressive stresses arise from domain mismatch and oxygen incorporated into the lattice. The oxygen levels present in the films deposited by RMS are determined to be low by SIMS analysis and so are the peak shifts observed in Raman and FTIR spectroscopy. Therefore, the compressive residual stresses in the films deposited by RMS are low. The peak shift measured in AlN films deposited by PLD at higher deposition temperature of 750 °C is low although no SIMS analysis was carried out. We believe these films deposited at 750 °C contain less oxygen and stresses are also relaxed. On the contrary, the SIMS analysis of the films deposited by PLD at substrate deposition temperature of 600 °C showed higher oxygen levels and the resulting FTIR absorption peak shift was high, from unstressed value of 665 cm^{-1} to stressed value of 706 cm^{-1}. The resulting stresses are compressive to an estimated value of 30 GPa as shown in Table II. Previous work on reactive sputtered AlN films at different temperatures have not presented the SIMS analysis of oxygen levels.[4–12] However, since the AlN films were deposited under ultrahigh predeposition vacuum conditions, we expect the oxygen level to be fairly low unless the gas mixture contained oxygen impurities. These results allow us to conclude that lower substrate deposition temperature (600 °C) and lower vacuum conditions created by oxygen from the target used in deposition of AlN films by PLD were responsible for higher compressive residual stresses. AlN films deposited by RMS do not exhibit high oxygen level and therefore the films are subjected to much smaller compressive residual stress. The higher silicon levels in AlN films deposited by both PLD and RMS result from fast diffusion of silicon along grain boundaries in the columnar structure of textured films on Si(111) substrate.

Wear resistance associated with the AlN films deposited by PLD and RMS also reflects the presence of residual compressive stress. The higher wear resistance exhibited by AlN films deposited by PLD at 600 °C and containing higher oxygen level is associated with the higher compressive residual stress present in the film and therefore higher hardness. The films deposited at 600 °C by RMS with lower oxygen level and lower residual compressive stress also possess lower hardness. The adhesion strength of the films deposited by PLD at 600 °C is found to be low from the microscopic observations of wear tracks in wear test and the peeled regions near the wear tracks in the scratch test. In comparison, such regions are observed to be smooth around the wear tracks on the films deposited by RMS and the films are strongly adherent to the substrate. Therefore, the wear resistance offered by AlN films deposited by PLD is higher in the initial stages of wear because of the higher hardness but becomes low when the films delaminate in the second stage of wear. The opposite is true with respect to the wear behavior of AlN films deposited by RMS since the hardness of the films is lower but the adhesion strength is higher compared to the films deposited by PLD at the same substrate temperature.

V. SUMMARY AND CONCLUSIONS

AlN films were deposited on Si(111) substrates by PLD from an aluminum nitride target or by RMS from an aluminum target in the plasma of nitrogen and argon. Films deposited at substrate temperature between 300 and 750 °C by both methods were characterized by various techniques. AlN films were highly textured with AlN(0002)//Si(111) and grain size in the range of 20–40 nm. Films deposited by PLD and RMS exhibited larger broadening because of smaller grain size and textured nature of the film growth. Raman and FTIR spectroscopy illustrated that both crystalline and amorphous phases of AlN were present with the volume fraction of the later increased for lower substrate temperatures. The results also showed that the films are subjected to residual compressive stress.

The magnitude of compressive stress evaluated from the peak shift showed that the films deposited by pulsed laser deposition at 600 °C are subjected to a high compressive stress of 30 GPA while the films deposited by reactive magnetron sputtering at the same substrate temperature were under a residual compressive stress of 5 GPa. Secondary ion mass spectrometry showed that the films deposited by pulsed laser deposition at a temperature of 600 °C contained higher oxygen level in comparison with the films deposited by reactive magnetron sputtering. The presence of the high residual compressive stress in the films deposited by laser ablation method is attributed to higher oxygen incorporated from the target. The films deposited by reactive magnetron sputtering contained lower oxygen levels and therefore the residual stress was also low. The higher wear resistance and lower adhesion strength of the AlN films on Si(111) substrate deposited by pulsed laser deposition in comparison with the films deposited by reactive magnetron sputtering were also attributed to the higher residual compressive stress present in the films as a result of oxygen incorporation. The present effort has clearly illustrated that oxygen impurity levels are an important factor in the growth of AlN films by any method. Deposition of AlN films has clearly illustrated that oxygen impurity level is reduced in the RMS and as a result the residual stresses are lowered. Thus RMS is better suited for large area deposition of AlN films. The higher

silicon levels in the films deposited on Si(111) substrates can be reduced when the grain boundaries are eliminated by growth of epitaxial single crystalline films at higher temperature. Further improvements in the deposition of AlN films for optoelectronic applications are needed by increase of substrate temperature and use of ultrahigh vacuum conditions.

ACKNOWLEDGMENT

This research work is supported by Division of Design, Manufacture and Industrial Innovation of NSF.

[1]W. R. L. Lambrecht, Mater. Res. Soc. Symp. Proc. **339**, 565 (1994).
[2]P. Kung, A. Saxler, X. Zhang, D. Walker, T. C. Wang, I. Furguson, and M. Razeghi, Appl. Phys. Lett. **66**, 2958 (1995).
[3]K. S. Stevens, A. Ohtani, M. Kinniburgh, and R. Beresford, Appl. Phys. Lett. **65**, 321 (1994).
[4]R. D. Vispute, J. Narayan, H. Wu, and K. Jagannadham, J. Appl. Phys. **77**, 4724 (1995).
[5]R. D. Vispute, J. Narayan, and J. D. Budai, Thin Solid Films **299**, 94 (1997).
[6]M. G. Norton, P. G. Kotula, and C. B. Carter, J. Appl. Phys. **70**, 2871 (1991).
[7]K. Seiki, X. Xu, H. Okabe, J. M. Frye, and J. B. Halpern, Appl. Phys. Lett. **60**, 2234 (1992).
[8]S. R. Nishitani, S. Yoshimura, H. Kawata, and M. Yamaguchi, J. Mater. Res. **7**, 725 (1992).
[9]W. J. Meng, J. Heremans, and Y. T. Chang, Appl. Phys. Lett. **59**, 2097 (1991).
[10]I. Ivanov, L. Hultman, K. Jarrendahl, P. Martensson, J.-E. Sundgren, B. Hjorvarsson, and J. E. Greene, J. Appl. Phys. **78**, 5721 (1995).
[11]W. J. Meng, J. A. Sell, G. L. Eesley, and T. A. Perry, J. Appl. Phys. **74**, 2411 (1993).
[12]W. J. Meng, J. A. Sell, T. A. Perry, L. E. Rehn, and P. M. Baldo, J. Appl. Phys. **75**, 3446 (1994).
[13]G. K. Hubler, in *Pulsed Laser Deposition of Thin Films*, edited by D. B. Chrisey and G. K. Hubler (Wiley, New York, 1994), Chap. 13, p. 327.
[14]L. E. McNeil, M. Grimsditch, and R. H. French, J. Am. Ceram. Soc. **76**, 1132 (1993).
[15]C. Carlone, K. M. Lakin, and H. R. Shanks, J. Appl. Phys. **55**, 4010 (1984).
[16]J. A. Sanjurjo, E. Lopez-Cruz, P. Vogl, and M. Cardona, Phys. Rev. B **28**, 4579 (1983).
[17]D. R. McKenzie, D. Muller, and B. A. Pailthorpe, Phys. Rev. Lett. **67**, 773 (1991).
[18]G. Wei, J. Zi, K. Zhang, and X. Xie, J. Appl. Phys. **82**, 4693 (1997).
[19]R. Zarwasch, E. Rille, and H. R. Pulker, J. Appl. Phys. **71**, 5275 (1992).
[20]R. G. Wilson, F. A. Steve, and C. W. Magee, *Secondary Ion Mass Spectrometry*, A practical handbook for depth profiling and bulk impurity analysis (Wiley, New York, 1989), pp. App. F.4-F.5.
[21]A. U. Sheleg and V. A. Savastenko, Izv. Akad. Nauk SSSR, Neorg. Mater. **15**, 1598 (1979).
[22]A. Polian, M. Grimsditch, and I. Grzegory, J. Appl. Phys. **79**, 3343 (1996).
[23]Y. Takagi, M. Ahart, T. Azuhata, T. Sota, K. Suzuki, and S. Nakamura, Physica B **219&220**, 547 (1996).
[24]A. F. Wright, J. Appl. Phys. **82**, 2833 (1997).